Spiral-Defect Chaos in Rayleigh-Bénard Convection with Small Prandtl Numbers

Jun Liu and Guenter Ahlers
Department of Physics and Center for Nonlinear Science, University of California, Santa Barbara, California 93106
(Received 13 June 1996)

Rayleigh-Bénard convection is investigated for Prandtl numbers σ from 0.3 to 1.0 by using various pure gases and binary gas mixtures. The onset of spiral-defect chaos (SDC) moves to smaller values of $\epsilon \equiv R/R_c - 1$ (R is the Rayleigh number and R_c its critical value) as σ decreases. The measurements suggest that large-scale mean flows, which are expected to be stronger at smaller σ, play an important role in the spontaneous generation of SDC. SDC can occur and fully develop in the regime dominated by the Soret effect. [S0031-9007(96)01404-4]

PACS numbers: 47.54.+r, 47.20.Lz, 47.27.Te

Rayleigh-Bénard convection (RBC) occurs in a shallow horizontal fluid layer heated from below when the temperature difference ΔT exceeds a critical value ΔT_c. It has become a paradigm in the study of complex spatiotemporal behavior of nonequilibrium systems [1]. This is so because RBC lends itself to well controlled, quantitative experiments [2,3], and because there are calculations of secondary instabilities [4] which help in understanding the experimental results. The nature of the patterns which form for $\epsilon \equiv \Delta T/\Delta T_c - 1 > 0$ depends on the Prandtl number $\sigma \equiv \nu/\kappa$ (ν is the kinematic viscosity and κ the thermal diffusivity). Here we report on pattern formation over the important range $0.3 \lesssim \sigma \lesssim 1.0$, most of which had not been explored before.

An intriguing recent discovery [5] for $\sigma \simeq 1$ is *spiral-defect chaos* (SDC), a state consisting of small rotating spirals which appear, interact with each other and with other defects, and disappear, irregularly both in space and in time [see Figs. 2(b)–2(d) and 2(g) and 2(h) below]. Although giant cell-filling spirals had been observed before in RBC both in experiment [6] and in numerical solutions of model equations [7,8], it came as a surprise that SDC with its self-sustained chaotic dynamics and spatial complexity occurs in a parameter range where straight convection rolls are also stable [4]. Soon after its experimental discovery, SDC was found in numerical solutions of generalized Swift-Hohenberg equations [9,10] (which are models for RBC) and of the Navier-Stokes equations [11], as well as in several additional experiments [12–14]. Although there is only a partial framework for the understanding of SDC [10], simulations [7–10] show that large-scale mean flow plays a role in spiral generation and dynamics. The mean flow, with a length scale much greater than a typical convection-roll wavelength, is superimposed upon the short-wavelength rolls. It arises when vertical vorticity is driven by roll curvature and amplitude modulation [15]. The magnitude of the mean flow is predicted to be proportional to $1/\sigma$, and thus its interaction with the rolls is expected to be stronger at lower σ. To our knowledge, there have been no experiments on RBC with samples sufficiently large to sustain SDC for the interesting parameter range $\sigma \lesssim 0.9$. Using both pure gases and binary gas mixtures to cover the range $0.3 \lesssim \sigma \lesssim 1.0$, we find that the value ϵ_s of ϵ for the onset of SDC decreases dramatically with decreasing σ, supporting the idea that mean flow plays a key role in the spontaneous generation of spiral defects.

Prandtl numbers of pure gases generally are larger than the value $2/3$ derived from kinetic theory [16] for a rigid-sphere gas. Liquid metals have $\sigma \lesssim 0.03$, but we know of no classical pure fluids [17] with $0.03 \lesssim \sigma \lesssim 0.67$. However, in binary gas mixtures values of σ as low as 0.2 can be reached if the masses of the two components are very different from each other [18]. We used Ar, CO_2, and SF_6 to cover the range $0.69 \lesssim \sigma \lesssim 1.00$. The properties of these gases are well known [19]. With mixtures of He-SF_6, He-CO_2, and Ne-Ar we covered the range $0.30 \lesssim \sigma \lesssim 0.80$ by changing the mole fraction x of the heavier component and the pressure P. The parameters of the mixtures had to be obtained from a combination of kinetic theory [16,20], data in the literature [21], and our measurements of λ. In Table I we list the properties of our samples at onset and the measured and theoretical [22] critical Rayleigh numbers R_c and wave numbers k_c. The good agreement between experiment and theory for R_c and k_c of the mixtures shows that the properties were determined quite accurately. The vertical thermal diffusion time $t_v = d^2/\kappa$ for $d = 1.46$ mm is also given in Table I.

The temperature difference is expressed in terms of the Rayleigh number $R \equiv \alpha g d^3 \Delta T/\kappa\nu$ [$\alpha \equiv -(1/\rho)(\partial\rho/\partial T)_{P,x}$, ρ is the density, g the gravitational acceleration, and d the cell thickness]. For pure fluids, the onset of convection occurs at $R = R_{c0} = 1708$. In mixtures, there are concentration gradients when $R > 0$ (the Soret effect) which may enhance or retard the buoyancy. This effect is characterized by the separation ratio ψ. When $\psi > 0$ ($\psi < 0$), the induced concentration gradient is destabilizing (stabilizing) and $R_c < R_{c0}$ ($R_c > R_{c0}$). For our mixtures, $\psi > 0$ and convection at onset consists of time independent rolls [see Fig. 2(a)

 0031-9007/96/77(15)/3126(4)$10.00

TABLE I. Parameters of some runs. $\overline{T}$ is the mean temperature of the cell at $\Delta T = \Delta T_c$, and $k \equiv 2\pi d/\lambda$ the dimensionless wave number, where λ is the roll wavelength. The subscript c denotes the onset of convection, while superscripts t and e stand for the theoretical prediction and the measured value, respectively. See text for other notations.

Gas	x	P (bars)	$\overline{T}$(°C)	σ	L	ψ	t_v (s)	R_c^e/R_{c0}	R_c^t/R_{c0}	k_c^e	k_c^t
He-SF_6	0.19	28.09	22.53	0.30	0.71	0.80	1.14	0.23	0.26	2.4	2.4
He-SF_6	0.37	15.33	22.96	0.32	1.55	0.52	1.31	0.44	0.48	2.7	2.8
He-CO_2	0.52	30.60	23.99	0.46	1.72	0.30	1.79	0.62	0.62	2.9	2.9
He-CO_2	0.87	25.97	23.33	0.69	4.92	0.08	4.31	0.85	0.89	2.9	3.1
Ne-Ar	0.66	36.65	26.07	0.64	1.09	0.03	2.58	0.88	0.92	2.8	3.1
Ar		29.73	23.45	0.69			3.12	1.00	1.00	3.1	3.1
SF_6		4.95	23.00	0.79			3.44	0.97	1.00	3.1	3.1
CO_2		24.92	21.46	0.90			6.64	0.99	1.00	3.1	3.1

below] similar to those of pure fluids. Another important parameter for mixtures is the Lewis number $L = D/\kappa$, where D is the mass diffusivity. For liquids $L \simeq 10^{-2}$, but for gases $L \simeq 1$.

The apparatus was described in Ref. [3]. We used two convection cells with $\Gamma \equiv r/d = 30$ ($r = 43.2$ mm, $d = 1.460$ mm) and $\Gamma = 70$ ($r = 42.3$ mm, $d = 0.607$ mm). They consisted of a sapphire top plate, a diamond-machined aluminum bottom plate, and circular sidewalls made of porous filter paper. The plates were parallel to within 2 μm. The pressure was regulated to ± 0.005 bar. The top plate was held at a constant temperature regulated to ± 1 mK, while the bottom-plate temperature, regulated to ± 0.5 mK , was varied as the experimental control parameter. Convection patterns were imaged using the shadowgraph method [3].

The onset of convection was found from the Nusselt number N (the ratio of the effective thermal conductivity to the conductivity in the conduction state). An example is shown in Fig. 1. We allowed 2 to 6 h (over $2\Gamma^2 t_v$) at each ϵ for transients to decay before taking a time average of N. Above the onset, time-independent straight rolls were stable for small ϵ and were the starting point for investigating the evolution of patterns. Examples of patterns observed for a He-SF_6 mixture ($x = 0.37$, $\sigma = 0.32$) at various ϵ are given in the first column of Figs. 2(a)–2(d). The second column gives images at the same ϵ values for pure Ar ($\sigma = 0.69$) [Figs. 2(e)–2(h)]. At each ϵ the pattern in the mixture is more disordered than in Ar. For He-SF_6, the pattern acquired a slow time dependence involving dislocations generated in the cell center near $\epsilon = 0.03$. Figure 2(a) already shows several dislocations for $\epsilon = 0.07$. In Ar this slow dynamics did not begin until $\epsilon \simeq 0.07$. Essentially time-

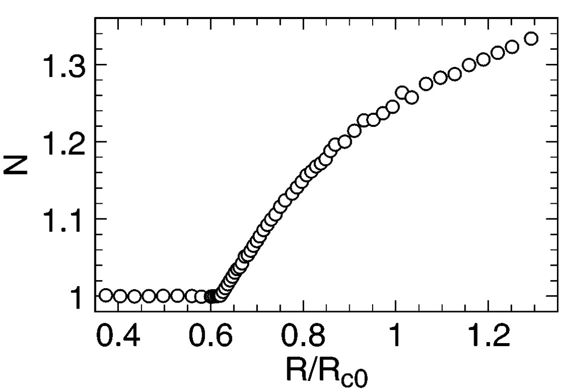

FIG. 1. Nusselt number as a function of the reduced Rayleigh number for $\Gamma = 30$ and He-CO_2 at $x = 0.52$ ($\sigma = 0.46$, $\psi = 0.30$, $L = 1.72$).

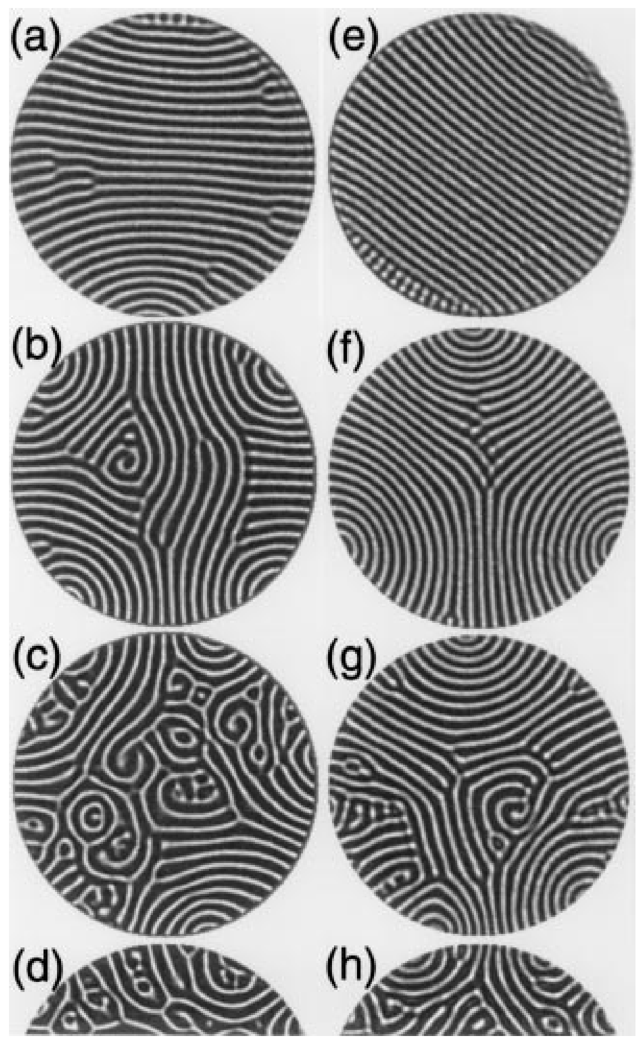

FIG. 2. Patterns for $\Gamma = 30$ in (a)–(d) He-SF_6 at $x = 0.37$ ($\sigma = 0.32$) and in (e)–(h) pure Ar ($\sigma = 0.69$), for $\epsilon = 0.07$ (a),(e), 0.2 (b),(f), 0.5 (c),(g), and 0.9 (d),(h).

independent straight rolls in Ar are shown in Fig. 2(e). As ϵ increased beyond 0.14, spirals appeared in the mixture, as illustrated in Fig. 2(b). In contrast, for ϵ up to 0.44, no spiral was observed in Ar, and the patterns consisted of two to three large sidewall foci [Fig. 2(f)]. When ϵ was large enough for spiral defects to appear in Ar [Fig. 2(g)], the patterns of He-SF_6 were already very chaotic, as shown in Fig. 2(c). When the pattern for Ar was full of spirals [Fig. 2(h)], those of He-SF_6 had become extremely disordered [Fig. 2(d)]. Thus we see that the erratic spatiotemporal dynamics develops at smaller ϵ in the lower-σ case.

We determined the onset value ϵ_s of SDC as a function of the Prandtl number *quantitatively*. Several diagnostics have been found to determine the onset of SDC [5,13,14]. In practice we found a simple spiral-counting method [14] to be easiest and most reliable, especially for the relatively small cell with $\Gamma = 30$. Because the generation of spirals was intermittent, especially for ϵ close to ϵ_s, we took data over 4 to 13 h (at least $3\Gamma^2 t_v$) at each ϵ to determine the time average $\bar{n}$ of spiral defects. Figure 3 gives $\bar{n}$ as a function of ϵ for one particular mixture. Since we do not know the functional form of $\bar{n}(\epsilon)$, we simply drew a smooth line through the data as shown, and determined its intercept ϵ_s with $\bar{n} = 0$. Since this procedure is somewhat subjective, relatively generous (also somewhat subjective) error bars were assigned to ϵ_s as shown in the figure. For σ near one this procedure agreed well with other methods [5,13]. To collect data for a single value of ϵ_s typically took 10 days.

Figure 4 shows ϵ_s as a function of σ for both gas mixtures (solid symbols) and pure gases (open symbols). The SDC occurs at lower ϵ for smaller σ. For $\Gamma = 30$ (circles) and the pure gases, ϵ_s dropped from 0.58 to 0.44 as σ was reduced from 0.9 to 0.69. For the mixtures and $\Gamma = 30$, ϵ_s was reduced from 0.44 to 0.10 as σ decreased from 0.69 to 0.30. It is known that the appearance of SDC depends on Γ. For CO_2 at $\sigma \approx 1$, $\epsilon_s \approx 0.55$ when $\Gamma = 40$ [13] while $\epsilon_s \approx 0.25$ when $\Gamma = 75$ [5]. Thus, we also made measurements in the cell with $\Gamma = 70$. The results are shown as triangles in Fig. 4. Near $\sigma = 1$, the rate at which ϵ_s decreases with σ seems nearly the same for the two values of Γ. However, for $\sigma \lesssim 0.8$ the dependence of ϵ_s on σ becomes very weak for $\Gamma = 70$. Close to our lower limit for σ ($\sigma \simeq 0.3$), the results for ϵ_s for the two cells come together again.

An obvious question is whether the Soret mechanism affects the onset of SDC. To answer it, we plot R_c and $R_s = R_c(1 + \epsilon_s)$ vs σ in Fig. 5 for $\Gamma = 30$. First, we consider the cases He-SF_6 at $x = 0.19$ and 0.37. As shown in Table I, their σ values (0.30 vs 0.32) are very close to each other, but their ψ values are very different (0.80 vs 0.52). Both R_c and R_s differ roughly by a factor of 2 (Fig. 5). However, the difference of their ϵ_s (Fig. 4) is small and consistent with the small difference of σ. Second, we look at the pair of runs for $\sigma = 0.69$ which are for pure Ar and for He-CO_2 at $x = 0.87$. The pure gas has no Soret effect ($\psi = 0$) while the mixture has $\psi = 0.08$. Their ϵ_s is the same (Fig. 4), although R_c and R_s differ substantially. It is clear that R_c and R_s depend on ψ, but ϵ_s is determined primarily by σ.

An interesting aspect of the results is that SDC can fully develop in the Soret regime $R < R_{c0}$, where the convection is strongly dependent on mass diffusion. For example, the disordered pattern shown in Fig. 2(d) was at $R/R_{c0} = 0.84$. In contrast, patterns in binary-liquid mixtures are ordered (square patterns or rolls) for $R \lesssim R_{c0}$ [23]. Whereas in liquid mixtures heat transport below R_{c0} is unobservably small, in gas mixtures significant heat can be transported in the Soret regime as shown in Fig. 1. For the case of Fig. 1, SDC occurred above $R/R_{c0} \approx 0.75$. There is no obvious signature in the Nusselt number at the SDC onset. When R is increased further, neither the convection patterns nor the heat transport undergo a qualitative change near R_{c0}.

We showed quantitatively that the onset of SDC is strongly affected by the Prandtl number. The experimental results in Fig. 4 provide a good argument for the essential role of large-scale mean flows in the spontaneous generation of spiral defects. We found that SDC can occur and fully develop in the regime dominated by the Soret mechanism. The critical value ϵ_s appears to be independent of

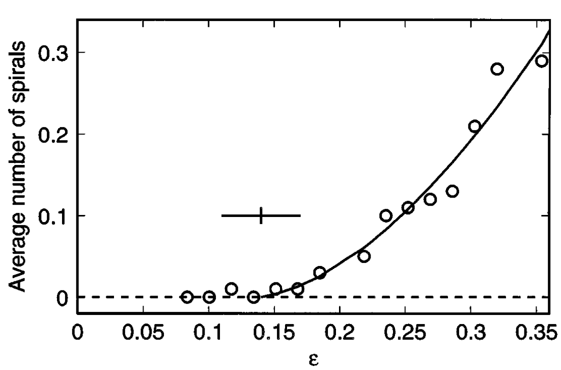

FIG. 3. Time average of the number of spirals for $\Gamma = 30$ and He-SF_6 at $x = 0.37$ ($\sigma = 0.32$) as a function of ϵ. The result $\epsilon_s = 0.14 \pm 0.03$ is indicated.

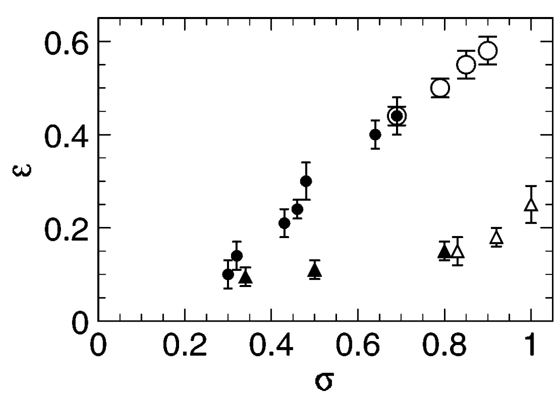

FIG. 4. Onset value ϵ_s for SDC as a function of σ. Open symbols: pure gases, solid symbols: mixtures, circles: $\Gamma = 30$, triangles: $\Gamma = 70$.

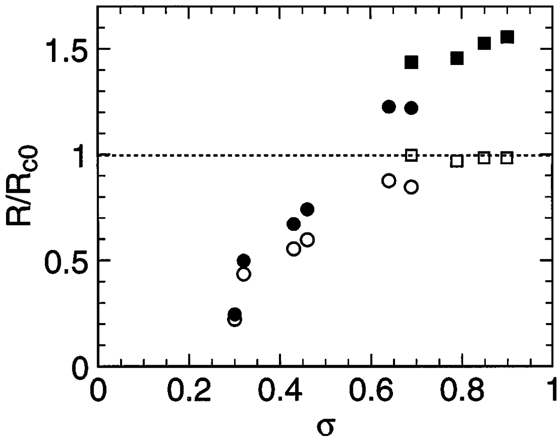

FIG. 5. Critical Rayleigh numbers R_c (open symbols) and Rayleigh numbers R_s at SDC onset (solid symbols) vs σ for $\Gamma = 30$. Circles: mixtures, squares: pure gases.

the Soret effect, but R_s is not. Hence the relative strength of mean flows is characterized by ϵ rather than by R.

Although the Prandtl number was tuned from 0.3 to 1.0, the behavior of $\epsilon_s(\sigma)$ outside this regime remains somewhat uncertain. It is difficult to do experiments in a large-Γ cell for σ significantly smaller than 0.3 (such as mercury at $\sigma \approx 0.025$); however, numerical simulations may be feasible. A naive linear extrapolation of the $\Gamma = 30$ data in Fig. 4 suggests that ϵ_s should vanish near $\sigma = 0.2$. However, the $\Gamma = 70$ data show that a smooth extrapolation to a finite value of ϵ_s at $\sigma = 0$ is more likely to be correct. Clearly, measurements for $\sigma < 0.3$ would be most useful. Quantitative results do not exist for $\sigma > 1$, though it was shown that there is a transition from SDC to a chaotic state dominated by targets near $\sigma \approx 3.5$ [12].

We thank David S. Cannell, Yu-Chou Hu, and Stephen W. Morris for many helpful discussions. We are grateful to Greg Swift for alerting us to the opportunity to reach small σ values in gas mixtures. This work was supported by the Department of Energy through Grant No. DE-FG03-87ER13738.

[1] See, for instance, M. C. Cross and P. C. Hohenberg, Rev. Mod. Phys. **65**, 851 (1993).
[2] V. Croquette, Contemp. Phys. **30**, 113, 153 (1989).
[3] J. R. de Bruyn, E. Bodenschatz, S. W. Morris, S. P. Trainoff, Y. Hu, D. S. Cannell, and G. Ahlers, Rev. Sci. Instrum. **67**, 2043 (1996).
[4] F. H. Busse, Rep. Prog. Phys. **41**, 1929 (1978).
[5] S. W. Morris, E. Bodenschatz, D. S. Cannell, and G. Ahlers, Bull. Am. Phys. Soc. **37**, 1734 (1992); Phys. Rev. Lett. **71**, 2026 (1993); Physica (Amsterdam) D (to be published).
[6] E. Bodenschatz, J. R. deBruyn, G. Ahlers, and D. S. Cannell, Phys. Rev. Lett. **67**, 3078 (1991).
[7] M. Bestehorn, M. Fantz, R. Friedrich, and H. Haken, Phys. Lett. A **174**, 48 (1993).
[8] H.-W. Xi, J. D. Gunton, and J. Viñals, Phys. Rev. E **47**, R2987 (1993).
[9] H.-W. Xi, J. D. Gunton, and J. Viñals, Phys. Rev. Lett. **71**, 2030 (1993).
[10] M. C. Cross and Y. Tu, Phys. Rev. Lett. **75**, 834 (1995).
[11] W. Decker, W. Pesch, and A. Weber, Phys. Rev. Lett. **73**, 648 (1994).
[12] M. Assenheimer and V. Steinberg, Phys. Rev. Lett. **70**, 3888 (1993); Nature (London) **367**, 345 (1994).
[13] Y.-C. Hu, R. E. Ecke, and G. Ahlers, Phys. Rev. E **48**, 4399 (1993); Phys. Rev. Lett. **74**, 391 (1995); Phys. Rev. E **51**, 3263 (1995).
[14] R. E. Ecke, Y.-C. Hu, R. Mainieri, and G. Ahlers, Science **269**, 1704 (1995).
[15] E. D. Siggia and A. Zippelius, Phys. Rev. Lett. **47**, 835 (1981); M. C. Cross and A. C. Newell, Physica (Amsterdam) **10D**, 299 (1984); H. S. Greenside, M. C. Cross, and W. M. Coughran, Jr., Phys. Rev. Lett. **60**, 2269 (1988); V. Croquette, P. LeGal, A. Pocheau, and R. Guglielmetti, Europhys. Lett. **1**, 393 (1986).
[16] J. O. Hirschfelder, C. F. Curtiss, and R. B. Bird, *Molecular Theory of Gases and Liquids* (John Wiley & Sons, New York, 1964).
[17] An exception is liquid helium. As the superfluid transition temperature is approached from above, σ vanishes. However, so far flow visualization has not been successful under the required cryogenic conditions.
[18] F. W. Giacobbe, J. Acoust. Soc. Am. **96**, 3568 (1994).
[19] See, for instance, V. A. Rabinovich, A. A. Vasserman, V. I. Nedostup, and L. S. Veksler, *Thermophysical Properties of Neon, Argon, Krypton, and Xenon* (Hemisphere, Washington, DC, 1988); Ref. [3].
[20] J. Kestin, K. Knierim, E. A. Mason, B. Najafi, S. T. Ro, and M. Waldman, J. Phys. Chem. Ref. Data **13**, 229 (1984); J. Bzowski, J. Kestin, E. A. Mason, and F. J. Uribe, J. Phys. Chem. Ref. Data **19**, 1179 (1990).
[21] A large number of papers is relevant. Here we cite only J. Kestin, Y. Nagasaka, and W. A. Wakeham, Physica (Amsterdam) **113A**, 1 (1982); R. DiPippo, J. Kestin, and K. Oguchi, J. Chem. Phys. **46**, 4758 (1967), as examples.
[22] W. Hort, S. J. Linz, and M. Lücke, Phys. Rev. A **45**, 3737 (1992); St. Hollinger and M. Lücke, Phys. Rev. E **52**, 642 (1995).
[23] E. Moses and V. Steinberg, Phys Rev. A **43**, 707 (1991); M. A. Dominguez-Lerma, G. Ahlers, and D. S. Cannell, Phys. Rev. E **52**, 6159 (1995).